SUPPLEMENTARY INFORMATION

Gogl et al.

Supplementary Table 1. Crystal structures of the 14-3-3/motif III peptide complexes available in the PDB. FSC – fusicoccin, cotA – cotylenin A, "modified" indicates that the peptide sequence or length are not authentic. Red bold font highlights the peptides matching the pS/pT**XX**-COOH motif III consensus.

PDB ID	Motif III peptide	(pS/pT)Xn-COOH, n=	14-3-3 partner	Complex contents	Resolution	Ref.
1O9D	..QSY**pT**V-COOH	1	PMA2	1433 + peptide	**2.30 Å**	1
1O9F	..QSY**pT**V-COOH	1	PMA2	1433 + peptide +FSC	**2.70 Å**	1
3E6Y	..QSY**pT**V-COOH	1	PMA2	1433 + peptide +cotA	**2.50 Å**	2
5NWI	..YFS**pS**N-COOH	1	KAT1	1433 + peptide	**2.35 Å**	3
5NWJ	..YFS**pS**N-COOH	1	KAT1	1433 + peptide	**2.07 Å**	3
5NWK	..YFS**pS**N-COOH	1	KAT1	1433 + peptide +FSC	**3.30 Å**	3
3IQU	.QRST**pS**T-COOH	1	Raf1 (modified)	1433 + peptide	**1.05 Å**	4
3IQV	.QRST**pS**T-COOH	1	Raf1 (modified)	1433 + peptide +FSC	**1.20 Å**	4
3P1N	.KRRK**pS**V-COOH	1	TASK-3	1433 + peptide	**1.40 Å**	5
3P1O	.KRRK**pS**V-COOH	1	TASK-3	1433 + peptide +FSC	**1.90 Å**	5
3P1P	.KRRK**pS**V-COOH	1	TASK-3	1433 mutant + peptide	**1.95 Å**	5
3P1Q	.KRRK**pS**V-COOH	1	TASK-3	1433 mutant + peptide +FSC	**1.70 Å**	5
3P1R	.KRRK**pS**V-COOH	1	TASK-3	1433 mutant + peptide	**1.70 Å**	5
3P1S	.KRRK**pS**V-COOH	1	TASK-3	1433 mutant + peptide +FSC	**1.65 Å**	5
3SMK	.KRRK**pS**V-COOH	1	TASK-3	1433 mutant + peptide +cotA	**2.10 Å**	5
3SML	.KRRK**pS**V-COOH	1	TASK-3	1433 mutant + peptide +FSC_deriv.	**1.90 Å**	5
3SMN	.KRRK**pS**V-COOH	1	TASK-3	1433 mutant + peptide +FSC_deriv.	**2.00 Å**	5
3SP5	.KRRK**pS**V-COOH	1	TASK-3	1433 mutant + peptide +cotA deriv.	**1.80 Å**	5
3SPR	.KRRK**pS**V-COOH	1	TASK-3	1433 mutant + peptide +FSC_deriv.	**1.99 Å**	5
3UX0	.KRRK**pS**V-COOH	1	TASK-3	1433 mutant + peptide +FSC_deriv.	**1.75 Å**	5
6GHP	.KRRK**pS**V-COOH	1	TASK-3	1433 mutant + FSC_deriv.	**1.95 Å**	6
3SMM	.KRRK**pS**V-COOH	1	TASK-3	1433 mutant + FSC_deriv.	**2.00 Å**	5
3SMO	.KRRK**pS**V-COOH	1	TASK-3	1433 mutant + FSC_deriv.	**1.80 Å**	5
4FR3	.KRRK**pS**V-COOH	1	TASK-3	1433 mutant + FSC_deriv.	**1.90 Å**	5
4JC3	.GFPA**pT**V-COOH	1	ERα	1433 + peptide	**2.05 Å**	7
4JDD	.GFPA**pT**V-COOH	1	ERα	1433 + peptide +FSC	**2.10 Å**	7
5N10	.GFPA**pT**V-COOH	1	ERα	1433 + peptide +ring stabilizer	**1.60 Å**	8
6HHP	.GFPA**pT**V-COOH	1	ERα	1433 + peptide +stabilizer 1	**1.80 Å**	9
6HMT	.GFPA**pT**V-COOH	1	ERα	1433 + peptide +stabilizer 2	**1.10 Å**	9
6HKB	.GFPA**pT**V-COOH	1	ERα	1433 + peptide +stabilizer 3	**1.70 Å**	9
6HKF	.GFPA**pT**V-COOH	1	ERα	1433 + peptide +stabilizer 4	**1.80 Å**	9
6HN2	.GFPA**pT**V-COOH	1	ERα	1433 + peptide +stabilizer 5	**1.70 Å**	9
6HMU	.GFPA**pT**V-COOH	1	ERα	1433 + peptide +stabilizer 6	**1.20 Å**	9
6W0L	SMRRM**pS**M-COOH	1	Henipah virus protein W	1433 + peptide	**2.30 Å**	10
4O46	**RTARpSKV-COOH**	**2**	**Influenza virus NS1**	**1433 + peptide**	**2.90 Å**	11
6TWZ	**RTRREpTQL-COOH**	**2**	**HPV16 E6**	**1433 + peptide**	**2.80 Å**	12
6T80	LRRN**pS**GCG-COOH	3	AANAT (modified)	1433σ-peptide chimera	**2.99 Å**	13

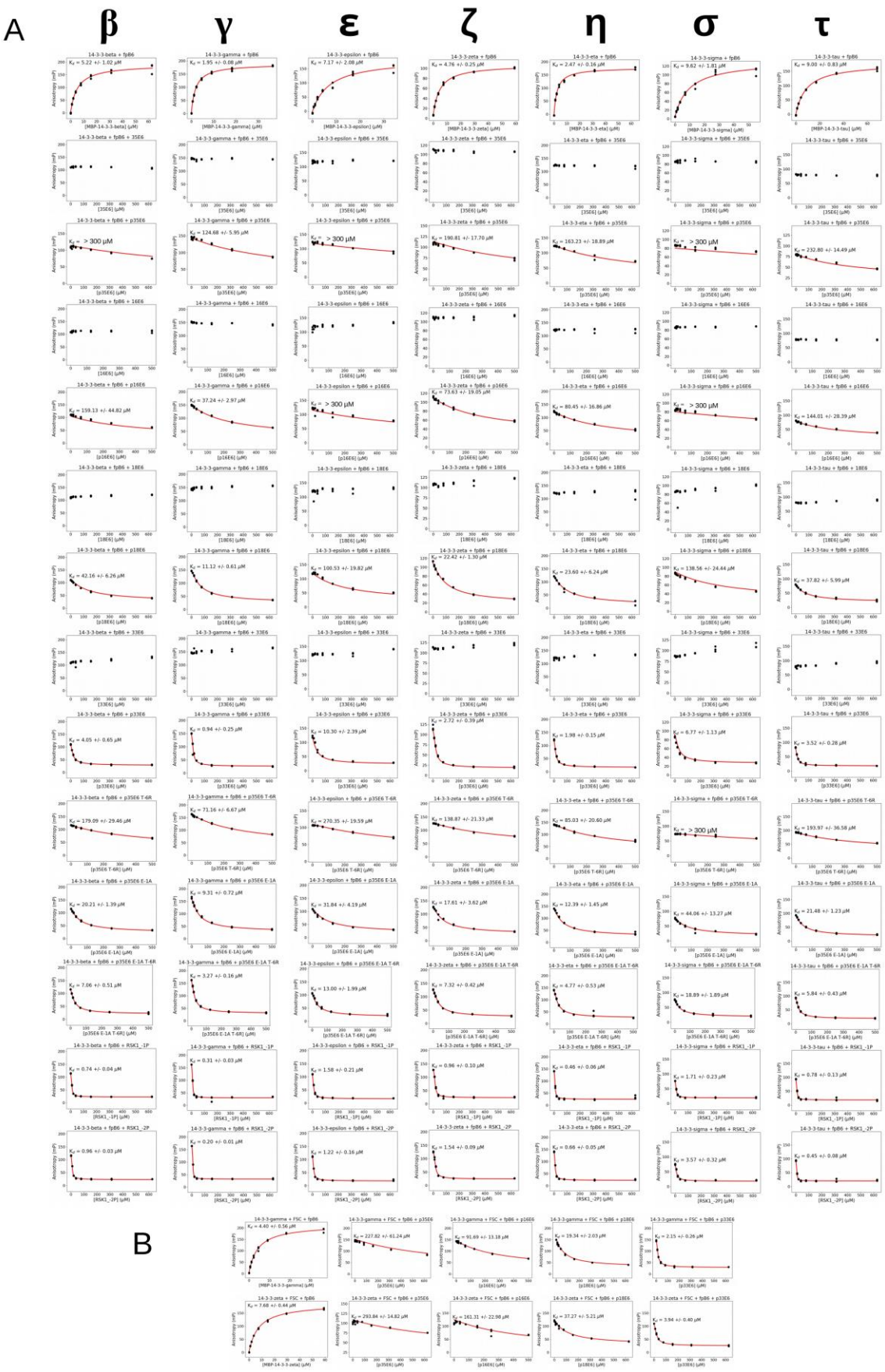

Supplementary figure 1. (see the legend on the next page)

Supplementary figure 1. Competitive FP measurements with the entire family of seven human 14-3-3 proteins. **A**. In each section, the first panel shows the direct FP experiments between the labeled peptide tracer and the titrated 14-3-3 protein and the following panels show competitive titrations. Competitive experiments were performed at a relatively high protein concentration to achieve 80% complex formation with the peptide tracer. Obtained polarization values were fitted with ProFit [14]. During competitive fitting, an experimental window close to the window of the direct experiment was either achieved without restraints or a restrained fitting was used. No fitted curve is shown if we did not observe a quantifiable competition. **B**. Direct and competitive FP experiments in the presence of FSC.

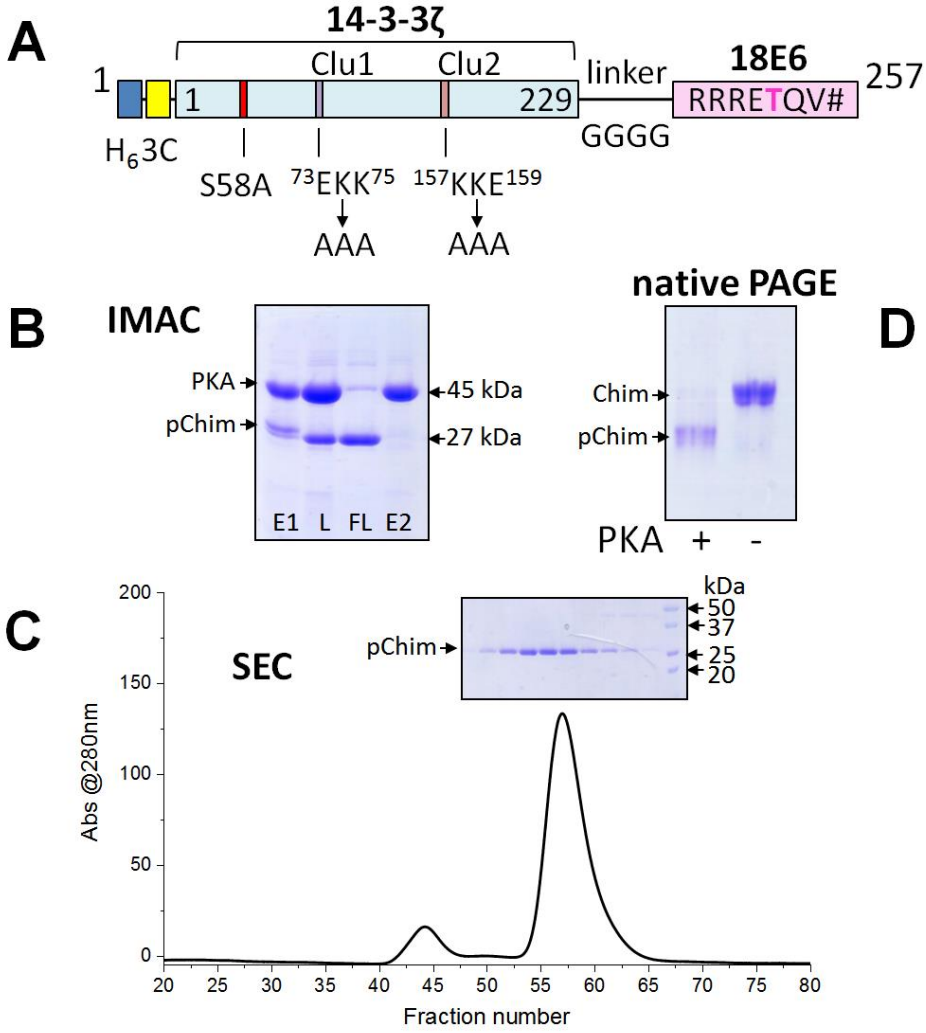

Supplementary figure 2. Design and purification of the 14-3-3ζ chimera with the 18E6 phosphopeptide. **A**. Schematic representation of the primary structure of the chimera. The His-tag (H6), 3C protease cleavage site (3C), 14-3-3ζ core modified to prevent phosphorylation of Ser58 and to promote crystallization by the surface entropy reducing mutations (highest scoring clusters 1 and 2 (clu1 and clu2, respectively) are marked [15, 16]), the GGGG linker and the 18E6 C-terminal phosphorylatable peptide are indicated (position of the phosphorylatable threonine is highlighted). The C-terminal carboxylic group is denoted by # and corresponds to the C-terminus of the 18E6 protein. **B**. Purification of the chimera bacterially co-expressed with the His-tagged catalytically active mouse PKA subunit by subtractive immobilized metal affinity chromatography (IMAC) analyzed by SDS-PAGE: E1 – fraction bound to the HisTrap HP column, L – E1 fraction proteolyzed by 3C and loaded on the HisTrap HP column again, FL – unbound fraction containing the untagged phosphorylated chimera, E2 – His-tag containing proteins bound to the column again. Positions of PKA and chimera as well as their apparent Mw values are shown by arrows. Note the downward shift of the chimera band due to 3C treatment. **C**. Size-exclusion chromatography (SEC) profile of the chimera on a Superdex 75 26/60 column (GE Healthcare) shown with the analysis of protein content of the main peak by SDS-PAGE. Arrows indicate positions of the chimera and Mw markers (shown in kDa). **D**. Native PAGE analysis of the purified chimera expressed in *E. coli* in the presence (+) or in the absence of PKA (-). Note the higher electrophoretic mobility of the phosphorylated chimera due to additional negative charges conferred by phosphate moiety.

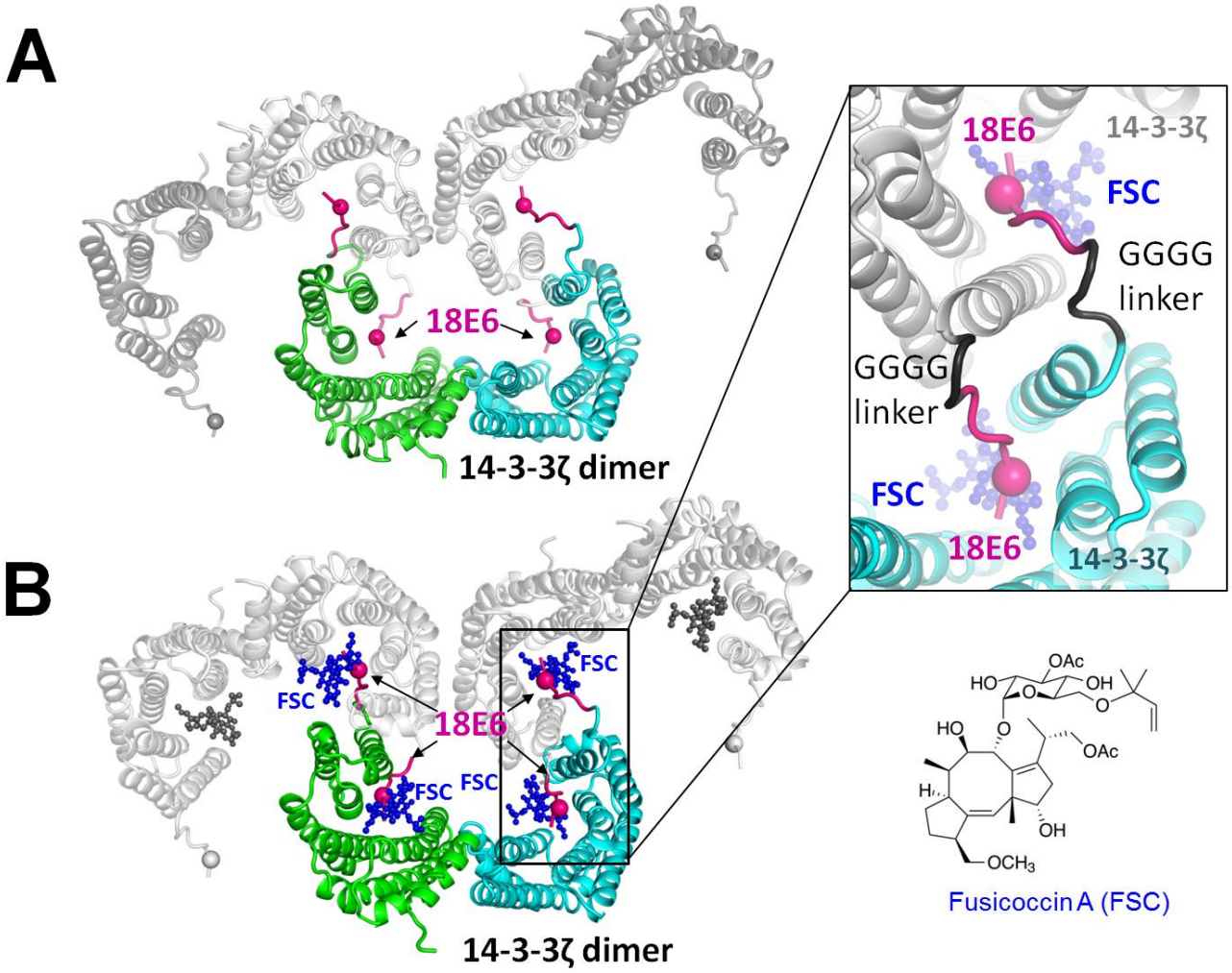

Supplementary figure 3. The arrangement of the chimera molecules in the crystal structures obtained in the absence (**A**) or in the presence of FSC (**B**). One 14-3-3ζ dimer of the asymmetric unit is colored, its crystallographically symmetric dimers are light grey. 18E6 phosphopeptides (magenta) are indicated by arrows, phospho-Thr residues are shown by spheres. The interdimer phosphopeptide swap stabilizing the supramolecular assembly is shown in a magnified view only for the FSC bound structure. A chemical formula of FSC is shown in the bottom-right corner.

Supplementary references

1. Wurtele M, Jelich-Ottmann C, Wittinghofer A, Oecking C. Structural view of a fungal toxin acting on a 14-3-3 regulatory complex. *EMBO J* **22**, 987-994 (2003).
2. Ottmann C, *et al.* A structural rationale for selective stabilization of anti-tumor interactions of 14-3-3 proteins by cotylenin A. *J Mol Biol* **386**, 913-919 (2009).
3. Saponaro A, *et al.* Fusicoccin Activates KAT1 Channels by Stabilizing Their Interaction with 14-3-3 Proteins. *Plant Cell* **29**, 2570-2580 (2017).
4. Molzan M, *et al.* Impaired binding of 14-3-3 to C-RAF in Noonan syndrome suggests new approaches in diseases with increased Ras signaling. *Mol Cell Biol* **30**, 4698-4711 (2010).
5. Anders C, *et al.* A semisynthetic fusicoccane stabilizes a protein-protein interaction and enhances the expression of K+ channels at the cell surface. *Chem Biol* **20**, 583-593 (2013).
6. Andrei SA, *et al.* Rationally Designed Semisynthetic Natural Product Analogues for Stabilization of 14-3-3 Protein-Protein Interactions. *Angew Chem Int Ed Engl* **57**, 13470-13474 (2018).
7. De Vries-van Leeuwen IJ, *et al.* Interaction of 14-3-3 proteins with the estrogen receptor alpha F domain provides a drug target interface. *Proc Natl Acad Sci U S A* **110**, 8894-8899 (2013).
8. de Vink PJ, Briels JM, Schrader T, Milroy LG, Brunsveld L, Ottmann C. A Binary Bivalent Supramolecular Assembly Platform Based on Cucurbit[8]uril and Dimeric Adapter Protein 14-3-3. *Angew Chem Int Ed Engl* **56**, 8998-9002 (2017).
9. Sijbesma E, *et al.* Site-Directed Fragment-Based Screening for the Discovery of Protein-Protein Interaction Stabilizers. *J Am Chem Soc* **141**, 3524-3531 (2019).
10. Edwards MR, *et al.* Henipavirus W Proteins Interact with 14-3-3 To Modulate Host Gene Expression. *J Virol* **94**, (2020).
11. Qin S, *et al.* Structural basis for histone mimicry and hijacking of host proteins by influenza virus protein NS1. *Nat Commun* **5**, 3952 (2014).
12. Gogl G, *et al.* Dual Specificity PDZ- and 14-3-3-Binding Motifs: A Structural and Interactomics Study. *Structure* **28**, 747-759 e743 (2020).
13. Sluchanko NN, Tugaeva KV, Titterington J, Antson AA. Unpublished work (2020).
14. Simon MA, *et al.* High-throughput competitive fluorescence polarization assay reveals functional redundancy in the S100 protein family. *FEBS J* **287**, 2834-2846 (2020).
15. Goldschmidt L, Cooper DR, Derewenda ZS, Eisenberg D. Toward rational protein crystallization: A Web server for the design of crystallizable protein variants. *Protein Sci* **16**, 1569-1576 (2007).
16. Goldschmidt L, Cooper DR, Derewenda ZS, Eisenberg D. SERp Server. (ed^(eds) (2007).